



## On partial slip flow and heat transfer of Non-Newtonian fluid due to a rotating porous disk

Lakshmi R<sup>1</sup>, Greeshma Joy<sup>2</sup>, Sanitha Shaji CS<sup>3</sup>

<sup>1</sup> Assistant Professor, Department of Mathematics, PSGR Krishnammal College for Women, Tamil Nadu, India

<sup>2,3</sup> Research Scholar, Department of Mathematics, PSGR Krishnammal College for Women, Tamil Nadu, India

### Abstract

In this article, partial slip flow and heat transfer of non-Newtonian fluid due to rotating porous disk is investigated. The Governing equations are solved numerically by using Runge - Kutta method of fifth order. The velocity and temperature profile is computed. The numerical calculations for wall roughness parameter ( $\lambda_1$  and  $\lambda_2$ ), Reiner - Rivlin fluid parameter (K) are also estimated. The effect of various non-dimensional parameter wall roughness ( $\lambda_1$  and  $\lambda_2$ ) in Newtonian and non-Newtonian fluid, Reiner - Rivlin fluid (K), Prandtl number (Pr), thermal slip ( $\gamma$ ) on velocity and temperature profile are analyzed through graphs.

**Keywords:** heat transfer, non-newtonian fluid, partial slip, rotating disk, von karman flow

### Introduction

The steady incompressible flow elicited by the rotation of an infinite plane with uniform angular rate is a certain resolution of the Navier - Stokes equations, as was initially described by T. von - Karman (1921) <sup>[1]</sup>. The flow is characterized by the dearth of a radial pressure gradient concerning the disk to balance the centrifugal forces therefore the fluid spirals outwards. The disk acts as a centrifugal fan, the fluid emanating from the disk being replaced by an axial flow directed back towards the surface of the disk. M. Turkyilmazoglu (2012) <sup>[2]</sup> explored stagnation-point flow because of stretchable rotating disk within the existence of thwart wise magnetic field. M. Turkyilmazoglu and P. Senel, (2013) <sup>[3]</sup> extended from the standard Von Karman swirling flow problem wherever the rotating disk surface admits partial slip in the presence of an identical suction or injection.

The MHD steady flow of viscous Nano fluid because of a rotating disk has been investigated by T. Hayat and M. Rashid (2015) <sup>[4]</sup>. J.A. Khan, M. Mustafa, T. Hayat and A. Alsaedi (2016) <sup>[14]</sup> enforced Keller - Box methodology for magneto Nano fluid flow and heat transfer close to a rotating disk to compute similarity solutions of the matter. I. Mustafa, T. Javed and A. Ghaffari (2016) <sup>[6]</sup> investigated numerical resolution of heat transfer analysis in three dimensional physical phenomenon stagnation point flow of incompressible ferro fluid over a stretchable rotating circular disk within the presence of uniform external field. Von Karman problem of infinite rotating disk was extended for the case wherever the area on top of the rough disk is provided by an electrically conducting nano fluid by M. Mustafa (2017) <sup>[15]</sup>. Ahmadpour and Sadeghy (2013) <sup>[8]</sup> explored the von - Karman problem for Bingham fluids. Their analysis unconcealed that yield stress in Bingham fluid contributes to a growth in minimum force required to keep up steady disk rotation. Non-Newtonian physical phenomenon flow and heat transfer over an exponentially stretching sheet with partial slip boundary condition has been studied by B. Sahoo and S. Poncet, (2011) <sup>[9]</sup>.

The work of S. Han, L. Zheng, C. Li and X. Zhang (2014) <sup>[10]</sup>, the Coupled flow and heat transfer in elastic fluid with Cattaneo - Christov heat flux model with the help of homotopy analysis methodology (HAM). In porous medium, the flow and radiation heat transfer of a nanofluid over a stretching sheet with velocity slip and temperature jump was mentioned by L. Zhang, C. Zhang, X. Zhang and J. Zhang (2013) <sup>[11]</sup>. T. Javed and I. Mustafa (2016) <sup>[12]</sup> was investigated a mixed convection flow of a third - grade fluid close to the orthogonal stagnation point on a vertical surface with slip and viscous dissipation effects. The boundary layer flow of a second-grade fluid during a porous medium past a stretching sheet and heat transfer characteristics with power-law surface temperature or heat flux was studied by D.S. Chauhan and A. Olkha (2011) <sup>[13]</sup>.

S. Hina, M. Mustafa, T. Hayat and A. Alsaedi (2016) <sup>[14]</sup> explored the heat transfer characteristics within the peristaltic transport of Powell-Eyring fluid within a semicircular channel with compliant walls. The streamline flow of Oldroyd-B fluid evoked by a deforming sheet within the existence of transversal magnetic flux was mentioned by S. Abbasbandy, M. Mustafa, T. Hayat and A. Alsaedi (2017) <sup>[15]</sup>. Therefore the target of this present work is to study the partial slip flow and heat transfer of non-Newtonian Reiner - Rivlin fluid due to rotating disk. This present work is likely to possess concerning to the problem of heat transfer which may be helpful in industries for electrochemical systems, deposition of coatings on surfaces, rotor-stator system etc.

### 2. Mathematical Formulation

Let the steady flow of an incompressible Reiner-Rivlin fluid occupying semi-infinite region on top of an infinite disk coinciding with the plane  $z = 0$ . The disk is during a state of rigid body rotation regarding the vertical axis with constant angular velocity  $\omega$  through a porous medium that sets up a swirling flow within the neighboring fluid layers.

Let  $u$ ,  $v$  and  $w$  be the elements of velocity on the directions of accelerating  $r$ ,  $\phi$  and  $z$  severally. Due to the axial symmetry, the velocity elements are assumed to be independent of the angle coordinate  $u$ . Partial slip conditions are enforced considering that characteristic scale of protuberance is tiny compared to the boundary layer thickness. Let  $T_w$  be the constant temperature at the

disk and  $T_\infty$  is that the fluid temperature high above the surface. We tend to make use of the temperature jump condition is that the current analysis. Reiner and Rivlin have developed the subsequent represent relation:

$$\tau_{ij} = -p\delta_{ij} + \mu e_{ij} + \mu_c e_{ik} e_{kj}; \quad e_{jj} = 0, \quad (1)$$

in which  $\tau_{ij}$  denotes the strain tensor,  $p$  represents pressure,  $\mu$  is that the co-efficient of viscosity,  $\mu_c$  represents the cross-viscosity constant,  $\delta_{ij}$  is that the Kronecker symbol and  $e_{ij} = \left(\frac{\partial u_i}{\partial x_j}\right) + \left(\frac{\partial u_j}{\partial x_i}\right)$  is that the deformation rate tensor. Relevant equations describing fluid motion and heat transfer over a rotating disk are given below:

**Continuity Equation**

$$\frac{\partial u}{\partial r} + \frac{u}{r} + \frac{\partial w}{\partial z} = 0 \quad (2)$$

**Motion Equation**

$$\rho \left( u \frac{\partial u}{\partial r} + w \frac{\partial u}{\partial z} - \frac{v^2}{r} \right) = \frac{\partial \tau_{rr}}{\partial r} + \frac{\partial \tau_{rz}}{\partial z} + \frac{\tau_{rr} - \tau_{\phi\phi}}{r} \quad (3)$$

$$\rho \left( u \frac{\partial v}{\partial r} + w \frac{\partial v}{\partial z} + \frac{uv}{r} \right) = \frac{1}{r^2} \frac{\partial}{\partial r} (r^2 \tau_{r\phi}) + \frac{\partial \tau_{z\phi}}{\partial z} + \frac{\tau_{r\phi} - \tau_{\phi r}}{r} \quad (4)$$

$$\rho \left( u \frac{\partial w}{\partial r} + w \frac{\partial w}{\partial z} \right) = \frac{1}{r} \frac{\partial (r \tau_{rz})}{\partial r} + \frac{\partial \tau_{zz}}{\partial z} \quad (5)$$

**Energy Equation**

$$\rho c_p \left( u \frac{\partial T}{\partial r} + w \frac{\partial T}{\partial z} \right) = k \frac{\partial^2 T}{\partial z^2}, \quad (6)$$

where  $\rho$  stands for fluid density,  $k$  for thermal conduction and  $c_p$  for the specific heat capacity. The last term in Eq. (4) are often omitted by using symmetry assumption for the elements of stress tensor. For the current (axisymmetric) flow, the elements of deformation rate tensor are given below [8]:

$$\left. \begin{aligned} e_{rr} &= 2 \frac{\partial u}{\partial r}, & e_{\phi\phi} &= 2 \frac{u}{r}, & e_{zz} &= 2 \frac{\partial w}{\partial z}, \\ e_{r\phi} &= e_{\phi r} = r \frac{\partial}{\partial r} \left( \frac{v}{r} \right), & e_{z\phi} &= e_{\phi z} = \frac{\partial v}{\partial z}, \\ e_{rz} &= e_{zr} = \frac{\partial u}{\partial z} + \frac{\partial w}{\partial r} \end{aligned} \right\} \quad (7)$$

Through definition (1), the elements of stress tensor are obtained as follows:

$$\tau_{rr} = -p + \mu \left( 2 \frac{\partial u}{\partial r} \right) + \mu_c \left\{ 4 \left( \frac{\partial u}{\partial r} \right)^2 + \left( \frac{\partial v}{\partial r} - \frac{v}{r} \right)^2 + \left( \frac{\partial u}{\partial z} + \frac{\partial w}{\partial r} \right)^2 \right\} \quad (8)$$

$$\tau_{zr} = \mu \left( \frac{\partial u}{\partial z} + \frac{\partial w}{\partial r} \right) + \mu_c \left\{ \left( 2 \frac{\partial u}{\partial r} \right) \left( \frac{\partial u}{\partial z} + \frac{\partial w}{\partial r} \right) + \left( \frac{\partial v}{\partial r} - \frac{v}{r} \right) \left( \frac{\partial v}{\partial z} \right) + \left( \frac{\partial u}{\partial z} + \frac{\partial w}{\partial r} \right) \left( 2 \frac{\partial w}{\partial z} \right) \right\} \quad (9)$$

$$\tau_{\phi\phi} = -p + \mu \left( 2 \frac{u}{r} \right) + \mu_c \left\{ 4 \left( \frac{u}{r} \right)^2 + \left( \frac{\partial v}{\partial r} - \frac{v}{r} \right)^2 + \left( \frac{\partial v}{\partial z} \right)^2 \right\} \quad (10)$$

$$\tau_{r\phi} = \mu \left( \frac{\partial v}{\partial r} - \frac{v}{r} \right) + \mu_c \left\{ \left( 2 \frac{\partial u}{\partial r} \right) \left( \frac{\partial v}{\partial r} - \frac{v}{r} \right) + \left( \frac{\partial v}{\partial r} - \frac{v}{r} \right) \left( \frac{2u}{r} \right) + \left( \frac{\partial u}{\partial z} + \frac{\partial w}{\partial r} \right) \left( \frac{\partial v}{\partial z} \right) \right\} \quad (11)$$

$$\tau_{z\phi} = \mu \left( \frac{\partial v}{\partial z} \right) + \mu_c \left\{ \left( \frac{\partial v}{\partial r} - \frac{v}{r} \right) \left( \frac{\partial u}{\partial z} + \frac{\partial w}{\partial r} \right) + 2 \left( \frac{u}{r} \right) \left( \frac{\partial v}{\partial z} \right) + 2 \left( \frac{\partial v}{\partial z} \right) \left( \frac{\partial w}{\partial z} \right) \right\} \quad (12)$$

$$\tau_{zz} = -p + \mu \left( 2 \frac{\partial w}{\partial z} \right) + \mu_c \left\{ \left( \frac{\partial u}{\partial z} + \frac{\partial w}{\partial r} \right)^2 + \left( \frac{\partial v}{\partial z} \right)^2 + 4 \left( \frac{\partial w}{\partial z} \right)^2 \right\} \quad (13)$$

The partial slip condition for present flow is expressed as follows by assumptive no penetration at the disk.

$$\begin{aligned} u(r, 0) &= \beta_1 \tau_{rz}(r, 0), & v(r, 0) &= \beta_2 \tau_{z\phi}(r, 0) + r\omega, & w &= w_0 \\ T(r, 0) &= T_w + \beta_3 T_z(r, 0). \end{aligned} \tag{14a}$$

In which  $\beta_1$  denotes the radial slip coefficient,  $\beta_2$  is the azimuthal slip coefficient and  $\gamma$  represents the thermal slip coefficient. Since lateral velocities and temperature distinction are zero removed from the disk thus we have

$$u(r, z) \rightarrow 0, \quad v(r, z) \rightarrow 0, \quad T(r, z) \rightarrow T_\infty \text{ as } z \rightarrow \infty \tag{14b}$$

Let us outline the subsequent self-similar transformations in terms of dimensionless distance  $\zeta = (\omega/\nu)^{1/2}$

$$\begin{aligned} (u, v, w) &= (r\omega F'(\zeta), r\omega G(\zeta), -2\sqrt{\nu\omega}F(\zeta)) \\ (p, T) &= (p_\infty - \omega\mu P(\zeta), T_\infty + (T_w - T_\infty)\theta(\zeta)), \end{aligned} \tag{15}$$

Where prime indicates differentiation with respect to  $\zeta$ . Note that Eq. (2) is identically satisfied by transformations (15) and (3) convert into the subsequent ordinary differential equations

$$F''' - F'^2 + 2FF'' + G^2 + K(F''^2 - 2F'F''' - G'^2) = 0 \tag{16}$$

$$G'' - 2F'G + 2FG' + 2K(F''G' - F'G'') = 0 \tag{17}$$

$$\theta'' + 2PrF\theta' = 0 \tag{18}$$

In the above equations,  $pr = \frac{\mu c_p}{k}$  denotes the Prandtl number and  $K = \frac{\mu c \omega}{\mu}$  is material parameter of Reiner-Rivlin fluid. Let us define:

$$\lambda_1 = \rho(\omega\nu)^{1/2}\beta_1, \quad \lambda_2 = \rho(\omega\nu)^{1/2}\beta_2, \quad \gamma = \rho(\omega\nu)^{1/2}\beta_3 \tag{19}$$

Using (15), the boundary conditions (14a) and (14b) transform into the subsequent forms:

$$\left. \begin{aligned} F'(0) &= \lambda_1[F''(0) - 2KF'(0)F''(0)] \\ G(0) &= \lambda_2[G'(0) - 2KG'(0)F'(0)] + 1 \\ \theta(0) &= 1 + \gamma\theta'(0) \end{aligned} \right\} \tag{20a}$$

$$F' \rightarrow 0, G \rightarrow 0, \theta \rightarrow 0 \text{ as } \zeta \rightarrow \infty \tag{20b}$$

The presence of viscosity close to the disk produces tangential stress at the disk that resists its rotation. Torque  $T_0$  required to keep up steady rotation of disk with radius  $R$  is measured through the definite integral.

$$T_0 = - \int_0^R \tau_{z\phi}|_{z=0} (2\pi r^2) dr = - \frac{\pi\rho\omega}{2} \sqrt{\nu\omega} R^4 G'(0) \tag{21}$$

Quantity of prime interest during this work is that the skin friction coefficient  $C_f$  outlined as

$$C_f = \frac{\sqrt{\tau_r^2 + \tau_\phi^2}}{\rho(r\omega)^2} \tag{22}$$

where  $\tau_r$  and  $\tau_\phi$  denote the radial and azimuthal wall stresses. Through variables (15), Eq. (22) assumes the subsequent form:

$$C_f = \left(\frac{\omega r^2}{\nu}\right)^{-1/2} \sqrt{(F''(0))^2 + (G'(0))^2} \tag{23}$$

Another necessary quantity is the local Nusselt number  $Nu$  which may be obtained from the Fourier law as follows:

$$Nu = \frac{rq_w}{k(T_w - T_\infty)} = \left(\frac{\omega r^2}{\nu}\right)^{1/2} \theta'(0) \tag{24}$$

Additionally, the overall quantity of fluid drawn within the axial direction is measured through  $F(\infty)$ . Therefore numerical computations for  $F''(0), G'(0), \theta'(0)$  and  $F(\infty)$  will be made to grasp physical aspects of the problem.

### 3. Numerical Approach

Mathematical equati

$$x_1 = F, x_2 = F', x_3 = F'', x_4 = G, x_5 = G', x_6 = \theta, x_7 = \theta'$$

We acquire the subsequent

$$\begin{aligned} &= x_2, \quad x'_2 = x_3, \quad x'_3 = \frac{x_2^2 - 2x_1x_3 - x_4^2 - Kx_3^2 + Kx_5^2}{1 - 2Kx_2} \\ x'_4 &= x_5, \quad x'_5 = \frac{2x_2x_4 - 2x_1x_5 - 2Kx_3x_5}{1 - 2Kx_2} \\ x'_6 &= x_7, \quad x'_7 = -2Prx_1x_7 \end{aligned} \tag{25}$$

With the initial conditions

$$\begin{aligned} x_1(0) &= 0, & x_2(0) &= \lambda_1[x_3(0) - 2Kx_2(0)x_3(0)], \\ x_3(0) &= u(1), & x_4(0) &= \lambda_2[x_5(0) - 2Kx_5(0)x_2(0)] + 1, \\ x_5(0) &= u(2), & x_6(0) &= 1 + \gamma x_7(0), \\ x_7(0) &= u(3) \end{aligned} \tag{26}$$

To solve the above system numerically, we tend to implement Runge - Kutta methodology of fifth order considering appropriate guesses for the unknown slopes u(1), u(2) and u(3). Within the course of computations, the step size h = 0.01 is chosen whereas residual of boundary conditions at infinity is assumed to be 10<sup>-5</sup>.

### 4. Figures and Tables

**Table 1:** Comparison of present findings with those of Turkyilmazoglu and Senel [3] in uniform roughness case ( $\lambda_1 = \lambda_2$ ) with K=0

$\lambda_1$	$\lambda_2$	Existing $F''(0)$	Existing $G'(0)$	Existing $F(\infty)$	Present $F''(0)$	Present $G'(0)$	Present $F(\infty)$
0	0	0.5102332	-0.6159219	0.442228	0.5102336	-0.6159215	0.442225
1	1	0.1279241	-0.3949280	0.394713	0.1279245	-0.3949275	0.394709
5	5	0.0185883	-0.1433879	0.291842	0.0185887	-0.1433874	0.291838
10	10	0.0068125	-0.0810301	0.243797	0.0068129	-0.0810298	0.243794
20	20	0.0023615	-0.0437883	0.199904	0.0023619	-0.0437879	0.199901
40	40	0.0007899	-0.0229951	0.160963	0.0007904	-0.0229947	0.160958

**Table 2:** Computational results of  $F''(0), G'(0), F(\infty)$  and  $\sqrt{(F''(0))^2 + (G'(0))^2}$  for different values of  $\lambda_1, \lambda_2$  and K

$\lambda_1$	$\lambda_2$	K	$F(\infty)$	$F''(0)$	$G'(0)$	$\sqrt{(F''(0))^2 + (G'(0))^2}$
0	1	1	0.311704	0.207329	-0.358183	0.413860
1	1	1	0.344451	0.115543	-0.434951	0.450036
5	1	1	0.370578	0.046257	-0.495401	0.497560
10	1	1	0.377729	0.0269281	-0.512593	0.513299
20	1	1	0.382161	0.014733	-0.523514	0.523721
40	1	1	0.384368	0.007743	-0.529793	0.529849
1	0	1	0.391594	0.164951	-0.815802	0.832311
1	1	1	0.344451	0.115543	-0.434949	0.450034
1	5	1	0.259795	0.053219	-0.149823	0.158994
1	10	1	0.217803	0.033268	-0.083027	0.089444
1	20	1	0.164479	0.019744	-0.044250	0.048455
1	40	1	0.130638	0.011339	-0.023054	0.025689
1	1	0	0.394629	0.127918	-0.394921	0.415121
1	1	2	0.292083	0.077914	-0.424419	0.431511
1	1	4	0.224869	0.033993	-0.351567	0.353210
1	1	6	0.187210	0.020209	-0.304638	0.305307
1	1	8	0.166737	0.014229	-0.272427	0.272798

**Table 3:** Values of  $\theta'(0)$  for different values of  $K$ ,  $\gamma$  and  $Pr$  when  $\lambda_1 = \lambda_2 = 1$

$K$	$\gamma$	$Pr$	$\theta'(0)$
0	1	8	0.533149
2	1	8	-0.453108
4	1	8	-0.370245
6	1	8	-0.322059
8	1	8	-0.289547
1	0	8	-1.003958
1	1	8	-0.500984
1	5	8	-0.166772
1	10	8	-0.090935
1	20	8	-0.047625
1	40	8	-0.024388
1	1	3	-0.343427
1	1	4	-0.394306
1	1	8	-0.500985
1	1	11	-0.544936

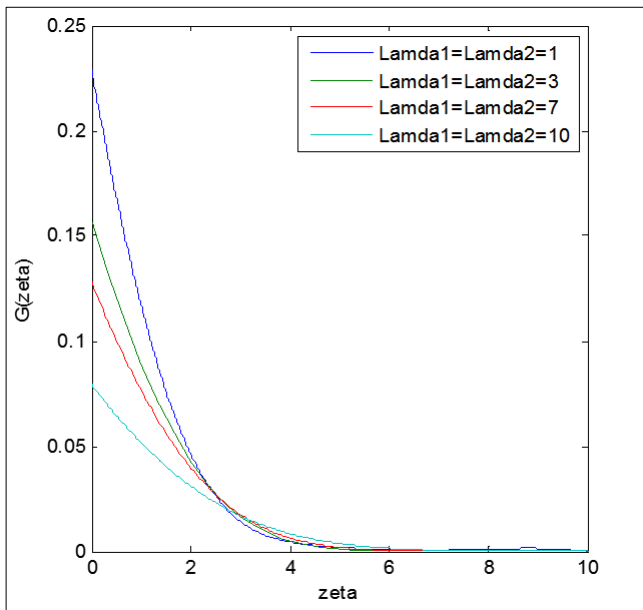


**Fig 1:** Velocity profile for different values of wall roughness parameters  $\lambda_1$  and  $\lambda_2$  in Newtonian fluid case

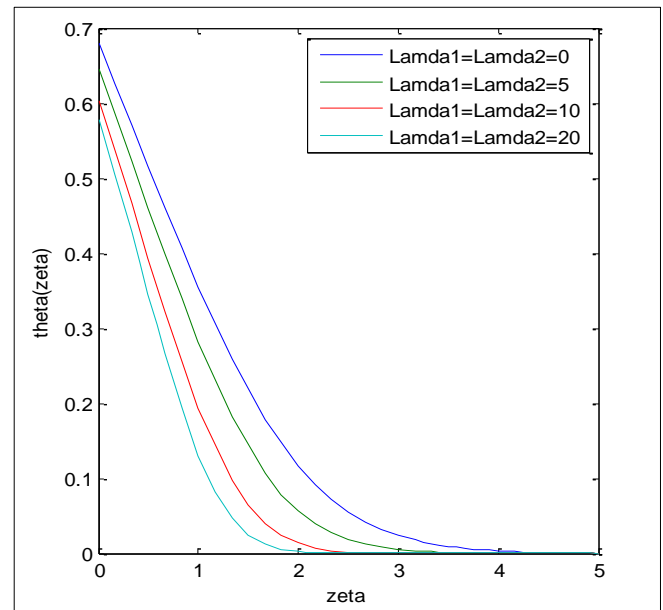


**Fig 2:** Temperature profile for different values of wall roughness parameters  $\lambda_1$  and  $\lambda_2$  in Newtonian fluid case

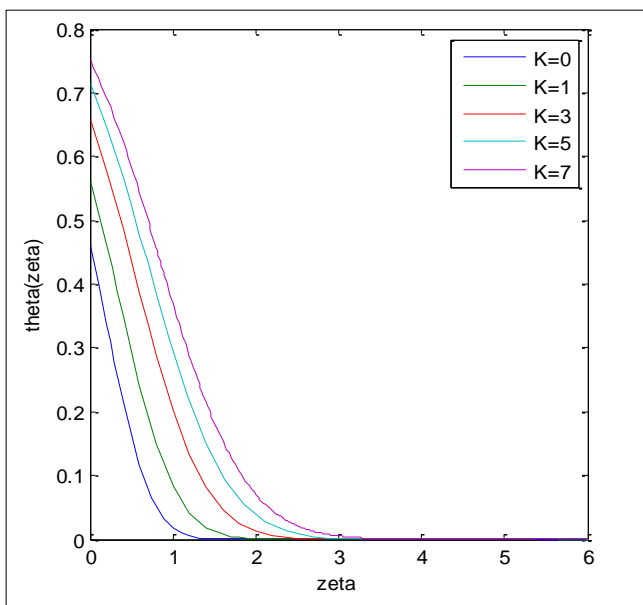


**Fig 3:** Temperature profile for different values of Reiner - Rivlin fluid parameter  $K$

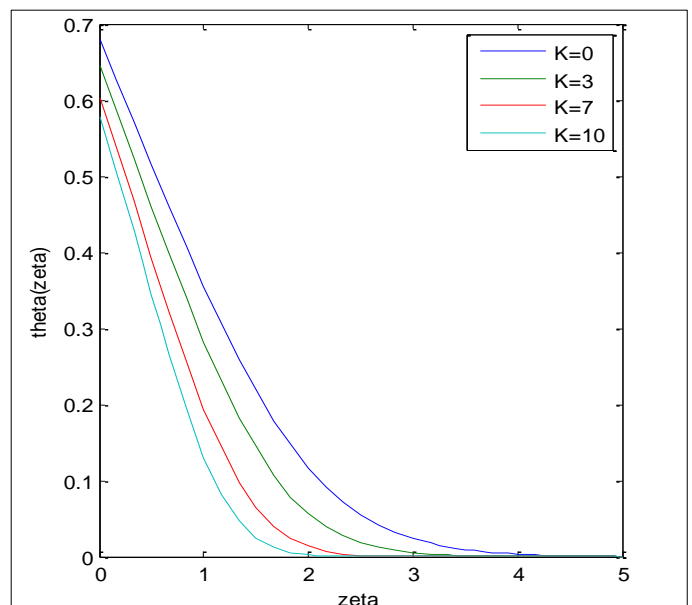


**Fig 4:** Temperature profile for different values of Reiner - Rivlin fluid parameter  $K$  in no - slip case

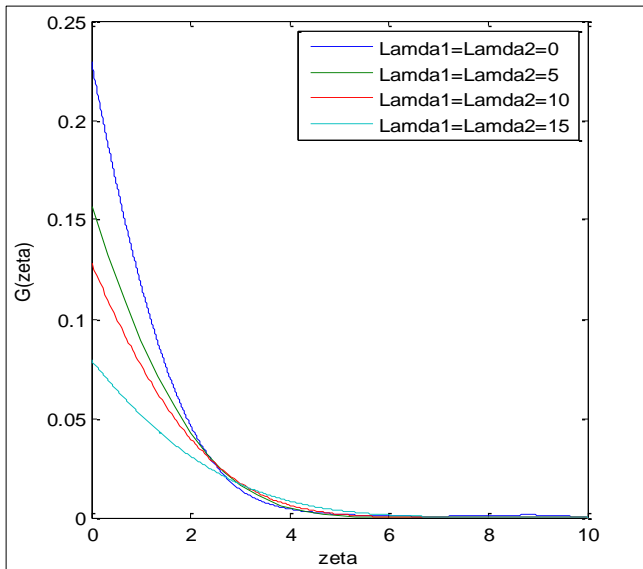


**Fig 5:** Velocity profile for different values of wall roughness parameters  $\lambda_1$  and  $\lambda_2$  in non - Newtonian fluid case

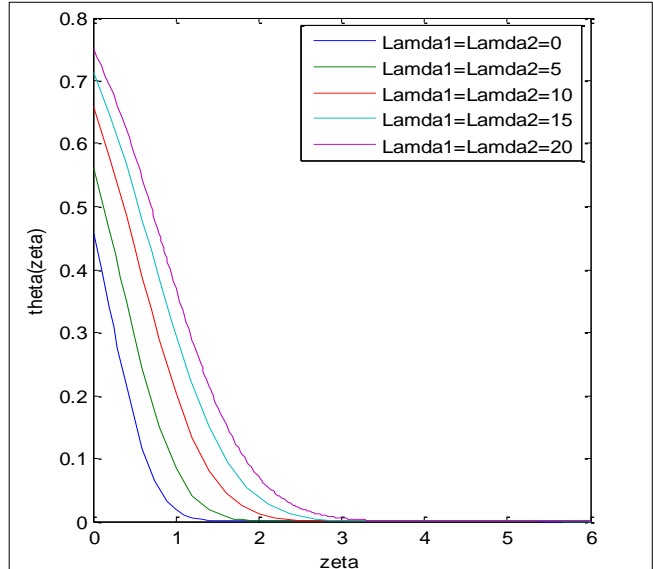


**Fig 6:** Temperature profile for different values of wall roughness parameters  $\lambda_1$  and  $\lambda_2$  in non - Newtonian fluid case

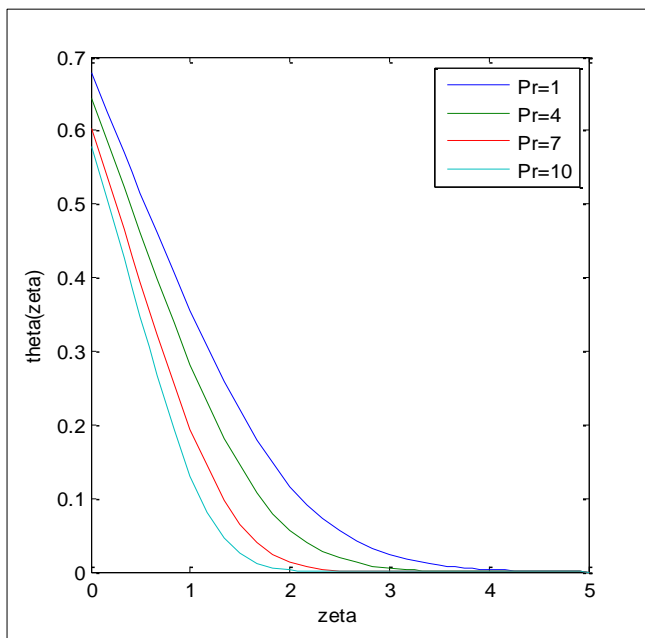


**Fig 7:** Temperature profile for different values of Prandtl number

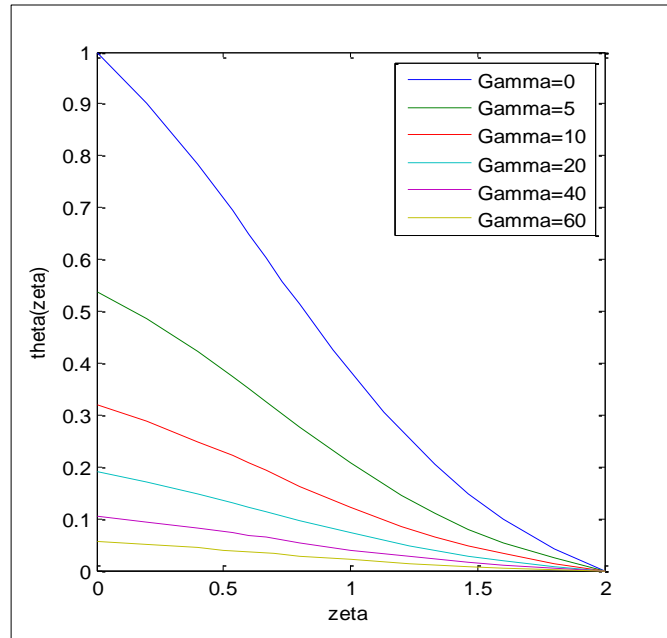


**Fig 8:** Temperature profile for different values of Thermal slip parameter

**5. Result and Discussion**

Effects of varied non - dimensional parameter wall roughness ( $\lambda_1$  and  $\lambda_2$ ) in Newtonian and non - Newtonian fluid, Reiner - Rivlin fluid (K), Prandtl number(Pr), thermal slip ( $\gamma$ ) on velocity and temperature profile are mentioned and examined graphically. Table 1 show the impact of wall roughness parameters and comparing the computational results of radial wall stress  $F''(0)$ , azimuthal wall stress  $G'(0)$  and entrainment velocity  $F(\infty)$  by the numerical theme is formed by with obtainable study [3] within the Newtonian fluid case. It demonstrates that our numerical findings are nearly the same as those found by [3] for all values of wall roughness parameters.

Table 2 computes  $F''(0)$ ,  $G'(0)$  and  $F(\infty)$  for numerous parameter values. In either radial or azimuthal slip coefficient incremented once torque furthermore because the skin friction factor elevates. The local Nusselt number obtained at completely different values of Reiner-Rivlin fluid parameter K and thermal slip parameter  $\gamma$  includes in table 3. It can increase elasticity parameter K then heat transfer rate ought to be elevate. The heat penetration depth shortens when thermal slip coefficient will increases and additionally Prandtl number Pr will increases once the heat transfer rate elevates. In figure 4.1 depicts the dimensionless velocity profile for various values of the wall roughness parameters  $\lambda_1$  and  $\lambda_2$  in Newtonian fluid case. It is detected that a rise in wall roughness parameters lead to decrease within the velocity profile.

In figure 4.2 illustrates the impact of wall roughness parameters  $\lambda_1$  and  $\lambda_2$  in Newtonian fluid case on the temperature profile. It shows that temperature component increases with a rise within the wall roughness parameters. In figure 4.3 the effect of Reiner - Rivlin fluid parameter K on temperature profile is shown. It is obvious that as K is enlarged, the temperature profile is magnified. In figure 4.4 for numerous values of Reiner - Rivlin fluid parameter K in no - slip case, its impact on temperature

profile is illustrated. It is additionally clear that because the value of Reiner – Rivlin fluid parameters increases, the temperature profile also increases.

In figure 4.5 indicates the fact that increase in wall roughness parameters  $\lambda_1$  and  $\lambda_2$  in non - Newtonian fluid case decelerates fluid flow within the Velocity profile. In figure 4.6 for various values of wall roughness parameters  $\lambda_1$  and  $\lambda_2$  in non - Newtonian fluid case, its result on the temperature profile are illustrated. It is also clear that as the value of wall roughness parameters increases, the temperature profile also increases. In figure 4.7 the result of Prandtl number on temperature profile is shown. It is obvious that as Pr is accrued, the temperature profile is weakened. In figure 4.8 for various values of Thermal slip parameter, its effect on the temperature profile are illustrated. It is additionally clear that because the value of thermal slip parameter increases, the temperature profile decreases.

## 6. Conclusion

In this study elasticity and wall roughness effects in Partial slip flow and heat transfer of non - Newtonian fluid evoked by a rough porous rotating disk is studied in the presence of suction. The consequences of viscoelasticity and wall roughness are examined numerically. The numerical resolution for determination governing nonlinear ordinary differential equation is executed through Runge-Kutta fifth order technique.

The Reiner-Rivlin fluid parameter K is incremented once radially outward flow close to the disk developed by disk centrifugal impact decrease. Decelerates driving torque and skin friction factor are expect for increasing elastic effects. The result of torque and skin friction factor are increasing by increasing wall roughness parameters  $\lambda_1$  and  $\lambda_2$ . The slip effect becomes stronger once the entrainment velocity reduces.

Radial velocity profile decreases close to the disk and also the wall roughness parameters elevates. The temperature profile is reciprocally proportional to the wall roughness parameters. Thermal boundary layer elevates for Reiner-Rivlin fluid parameter K values increases. Thermal slip parameter will increases once the thermal boundary layer shrinks and heat transfer rate enhances. Elastic impact enhances temperature profile however decreases the magnitude of local Nusselt number.

## 7. Acknowledgements

The authors are thankful to the learned referee for suggestions to improve the paper.

## 8. References

1. Von Kármán T. Über laminare und turbulente Reibung, Z. Angew. Math. Mech. ZAMM. 1921; 1:233-252.
2. Turkyilmazoglu M. Three dimensional MHD stagnation flow due to a stretchable rotating disk, Int. J Heat Mass Transf. 2012; 55:6959-6965.
3. Turkyilmazoglu M, Senel P. Heat and mass transfer of the flow due to a rotating rough and porous disk, Int. J Therm. Sci. 2013; 63:146-158.
4. Hayat T, Rashid M, Imtiaz M, Alsaedi A. Magnetohydrodynamic (MHD) flow of Cu-water nanofluid due to a rotating disk with partial slip, AIP Adv. 2015; 5. <https://doi.org/10.1063/1.4923380>, Article ID 067169.
5. Khan JA, Mustafa M, Hayat T, Alsaedi A. A revised model to study the MHD nanofluid flow and heat transfer due to rotating disk: numerical solutions, Neural Comput. Appl., 2016. <https://doi.org/10.1007/s00521-016-2743-4>.
6. Mustafa I, Javed T, Ghaffari A. Heat transfer in MHD stagnation point flow of a ferrofluid over a stretchable rotating disk, J. Molec. Liq. 2016; 219:526-532.
7. Mustafa M. MHD nanofluid flow over a rotating disk with partial slip effects: Buongiorno model, Int. J. Heat Mass Transf. 2017; 108:1910-1916.
8. Ahmadpour A, Sadeghy K, Swirling flow of Bingham fluids above a rotating disk: an exact solution, J. Non-Newton. Fluid Mech. 2013; 197:41-47.
9. Sahoo B, Poncet S. Flow and heat transfer of a third grade fluid past an exponentially stretching sheet with partial slip boundary condition, Int. J. Heat Mass Transf. 2011; 54:5010-5019.
10. Han S, Zheng L, Li C, Zhang X. Coupled flow and heat transfer in viscoelastic fluid with Cattaneo-Christov heat flux model, Appl. Math. Lett. 2014; 38:87-93.
11. Zhang L, Zhang C, Zhang X, Zhang J. Flow and radiation heat transfer of a nanofluid over a stretching sheet with velocity slip and temperature jump in porous medium, J. Franklin Inst. 2013; 350:990-1007.
12. Javed T, Mustafa I. Slip effects on a mixed convection flow of a third-grade fluid near the orthogonal stagnation point on a vertical surface, J. Appl. Mech. Tech. Phys. 2016; 57:527-536.
13. Chauhan DS, Olkha A. Slip flow and heat transfer of a second-grade fluid in a porous medium over a stretching sheet with power-law surface temperature or heat flux, Chem. Eng. Commun. 2011; 198:1129-1145.
14. Hina S, Mustafa M, Hayat T, Alsaedi A. Peristaltic flow of powell-eyring fluid in curved channel with heat transfer: a useful application in biomedicine, Comput. Meth. Prog. Biomed. 2016; 135:89-100.
15. Abbasbandy S, Mustafa M, Hayat T, Alsaedi A. Slip effects on MHD boundary layer flow of Oldroyd-B fluid past a stretching sheet: an analytic solution. J Brazilian Soc. Mech. Sci. Eng. 2017; 39:3389-3397.